Al-Qadisiyah Journal for Engineering Sciences 17 (2024) 029–037

Contents lists available at http://qu.edu.iq

Al-Qadisiyah Journal for Engineering Sciences

Journal homepage: https://qjes.qu.edu.iq

The influence of micro-channel shape filled by nanofluid on heat transfer characteristics: Numerical and experimental study

Abbas N. Tuaima *, Ahmed J. Shkarah, and Mohammed D. Salman

Department of Mechanical Engineering, College of Engineering, ThiQar University, Thi Qar, Iraq

ARTICLE INFO

Article history:
Received 05 October 2023
Received in revised form 10 January 2024
Accepted 28 February 2024

Keywords:
Microchannel
Heat sink
Circular cavity
Nanofluid
Dissipation

ABSTRACT

The integration of nanofluid effects and channel shape effects in a heat sink, which exhibits both variable and constant cross-section, has gained significant traction as an efficient cooling method for thermal devices, particularly microelectronic devices. This research presents an experimental and numerical analysis to compare the performance of microchannel heat sink designs (straight, zigzag, wavy, and circular cavities). In addition, the study dealt with the use of pure water and nanofluid (CuO-H2O) with volumetric concentrations of (0.01, 0.02, and 0.03) as coolants. COMSOL Multiphysics was used for numerical analysis to simulate and solve the problem of fluid and heat flow in 3D. The bottom wall of the four microchannels is subjected to a steady heat flux of 170 kW/m^2. The simulations were only performed within the laminar domain, encompassing a spectrum of Reynolds numbers ranging from 50 to 150. The influence on the microchannel's wall temperature, thermal resistance, pressure drop, and friction factor is exhibited. According to the findings, the wavy and zigzag microchannel heat sink cooled by nanofluid displays higher performance in terms of heat transmission and dissipation in comparison to the heat sink that was cooled by distilled water. as evidenced by a 12% increase in mussel number at volume concentrations of 0.03%.

1. Introduction.

During the latter part of the twentieth century, advancements in technology were observed across multiple disciplines, such as Engineering. These advancements encompassed the development of microreactors for hydrogen microfuel cells, lab-on-a-chip devices, and micro-total-analysis-systems (lTAS) in the field of biotechnology. Additionally, progress was made in the areas of Communications and Micro Devices. [1-6]. The phenomenon of overheating in these gadgets is attributed to the combination of constant downsizing and uninterrupted operation. Heat dissipation is a crucial consideration in many devices or machines to prevent potential harm to specific components. Elevated temperature levels can have adverse effects on the efficiency and lifespan of these devices, leading to energy wastage[7, 8]. Consequently, the integration of an efficient cooling system into their design has become imperative [9-12]. Heat dissipation is a significant challenge in numerous engineering applications. Microchannel heat dispersants are commonly employed to mitigate thermal fluxes from electrical components. In recent years, there have been significant advancements in precise manufacturing and assembly techniques, resulting in the emergence of a thriving sector of contemporary industrial technology often known as micro-electromechanical systems (MEMS).

MEMS systems have a distinct length scale between 1 mm and 1 µm. The cooling fluid plays a crucial role in cooling applications since it has a substantial impact on the cooling efficiency of the device. The optimization of cooling efficiency in a microchannel heat exchanger can be attained by judiciously choosing an appropriate fluid. Further investigation is warranted in this domain due to the proliferation of novel cooling fluids employed in recent times. The cooling systems exhibit a diverse range of geometric configurations in their microstructure, while the choice of working fluids can differ across different systems. The functionality and structural composition of the gadgets play a determining role. Hence, the categorization of cooling systems can be determined as either direct or indirect, depending on whether the operational liquid comes into direct

* *Corresponding author.*
E-mail address: abbas.n.t@utq.edu.iq (Abbas N. Tuaima)

https://doi.org/10.30772/qjes.2023.143746.1039

contact with the chip or the cooling component [13,14]. The preference for liquids in cooling applications is mostly attributed to their superior thermal characteristics compared to gases. In recent times, there has been a notable concentration of researchers on the utilization and formulation of nanofluids due to their inherent benefits. The superior heat transmission capability of nanofluids, as compared to conventional liquids, renders them the preferred option for coolant applications. The thermal conductivity shown by nanoparticles results in enhanced heat transfer properties. Furthermore, it has been shown that the surface area of nanoparticles is higher in solid substances as compared to fluid molecules. Additionally, nanoparticles demonstrate a notable degree of heat conductivity. To enhance the turbulent motion of nanoparticles inside a fluid, it is imperative to decrease the dimensions of those nanoparticles within the range of 1-100μm [15-22]. The primary objective of this study is to conduct forced convection experiments in order to examine and analyze the thermal performance characteristics of A microchannel heat sink. Experiments were conducted to get further heat transfer data about the effectiveness of utilizing nanofluids (CuO-H2O) as a coolant compared to pure water.

2. Description of the experimental configuration.

The schematic representation of the key parts of the open loop experimental facility in the current study is depicted in Fig. 1. The working fluid transitions from the tank to the annulus. When the valve is opened, the passage of clean water occurs through a filter that is exclusively employed when the working fluid is pure water only.

The temperature of the fluid in the upper tank of the test unit and the temperature of the incoming flow remain constant. The measurement of the volumetric flow rate within the open loop was conducted utilizing a flow meter. The test module's configuration, as shown in Fig. 1 is observable. The test section consists of several key elements, including a microchannel heat sink, cover plate, housing, microchannels, insulating layers, insulating block, and support plate. Figures 2 and 3 provide a schematic representation of the geometric configuration of the constructed straight microchannel heat sink. The whole dimensions are succinctly presented in Table 1. The microchannel heat sink was fabricated by machining eighteen parallel rectangular microchannels into a copper (Cu) block.

Four tiny holes were drilled along the centerline of the base of the heat sink on both sides. Two K-type thermocouples and pressure taps were strategically positioned to precisely measure the temperature rise and pressure drop at both the entrance and outflow of the microchannel heat sink. The measured quantities were documented by employing a digital temperature recorder to capture their respective values.

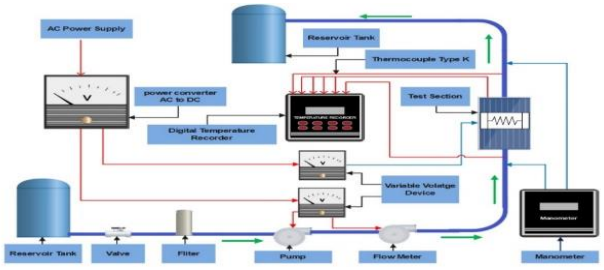

Figure 1. The experimental test facility's schematic.

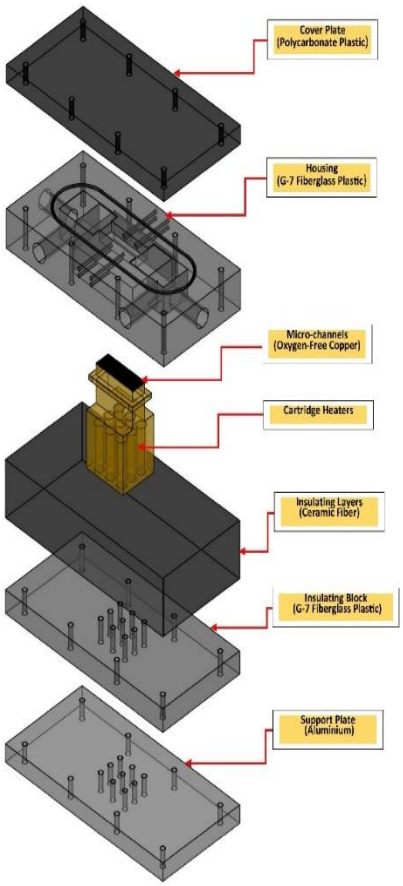

Figure 2. Test module configuration

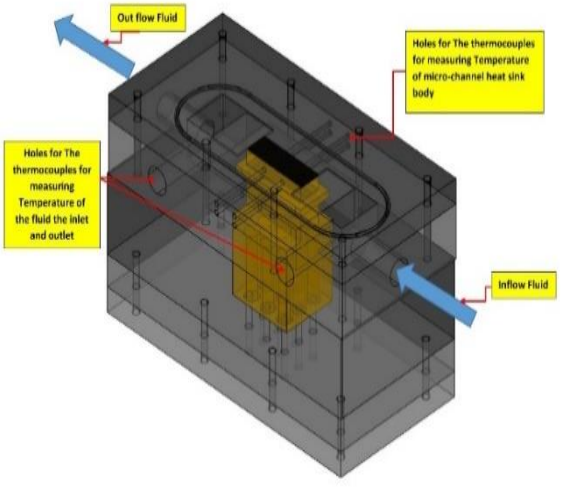

Figure 3. Test module configured

Table 1. The dimensions of the microchannel heat sink

Wm	Lm	Hm	Hc	Wc	Lc	X
10mm	30mm	990µm	720µm	270µm	30mm	270µm

3. Numerical analysis and verification.

This research presents a numerical investigation aimed at analyzing the thermal and flow characteristics of fluid flow within a heat sink. The heat sink under consideration consists of microchannels in various forms. The objective of this study is to elucidate the impact of different parameters on the performance of heat sinks and the efficiency of cooling systems. The factors under thorough investigation are those that exert an influence on the performance of the heat sink. The present study investigates the characteristics of a three-dimensional laminar flow, which is incompressible and steady-state. The flow consists of a single-phase fluid moving through several microchannels, while simultaneously undergoing conjugate heat transfer with a solid copper metal. The Naiver-Stock equation, the continuity equation, and the energy equation are the primary governing equations employed in both the mathematical and numerical solutions within this study.

The microchannel heat sink consists of many microchannels made of copper (Cu). The present study involved the examination and utilization of four distinct microchannels, each characterized by a different shape (straight, wavy, zigzag, and straight with circular cavities). The employment of a single symmetrical section of the micro-channel heat sink is employed in order to minimize computational time.

The first model The straight microchannel heat sink (SMHS) is characterized by a three-dimensional model with eighteen channels, all of which possess a uniform rectangular cross-sectional shape. The object is composed of copper stuff. The subsequent information outlines the geometric characteristics of a rectangular micro-channel heat sink. In order to save computational time, a unit consisting of a single channel and two symmetrical halves on either side of the channel, as depicted in Figure 3, has been chosen. The unit's dimensions are as follows: the unit length wall thickness (0.5wc) measures 0.135 mm, the channel width (wc) measures 0.27 mm, the channel length (Lc) measures 30 mm, and the channel height (Hc) measures 0.72 mm. The dimensions of the microchannel heat sink base are as follows: the heat sink width (Wm) measures 10 mm, and the heat sink length (Lm) measures 30 mm. Additionally, the base's bottom surface, as depicted in Fig. 1, receives a heat flux of 170 kW/m2.

The current study employs the Wavy microchannel heat sink (WMHS), as depicted in Fig. 2. This WMHS possesses identical dimensions to a conventional straight microchannel heat sink and comprises a total of seventeen wavy units. The profile of each wavy unit can be depicted using a combination of two circular arcs. Furthermore, Fig.3 illustrates a sinusoidal micro-channel characterized by an amplitude of A = 0.16mm and a fixed wavelength of λ = 0.16mm.

The current study employs the Wavy microchannel heat sink (WMHS), as depicted in Fig. 4. This WMHS possesses identical dimensions to a conventional straight microchannel heat sink and comprises a total of seventeen wavy units. The profile of each wavy unit can be depicted using a combination of two circular arcs. Furthermore, Fig.5 illustrates a sinusoidal micro-channel characterized by an amplitude of A = 0.16mm and a fixed wavelength of λ = 0.16mm.

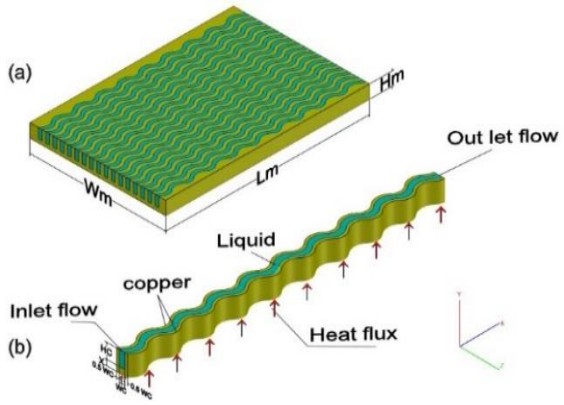

Figure 3. (a) Geometry of Straight microchannel heat sink, (b) Geometry of (SMHS) unit.

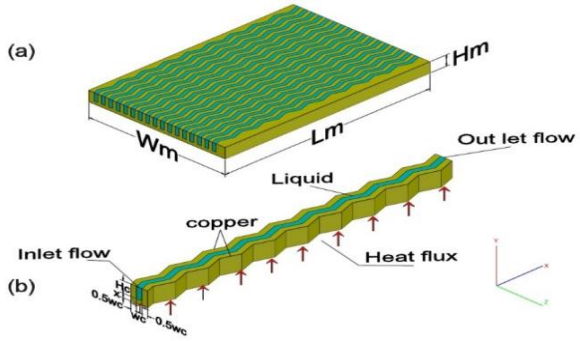

Figure 4. (a) Geometry of wavy microchannel heat sink, (b) Geometry of (WMHS) unit

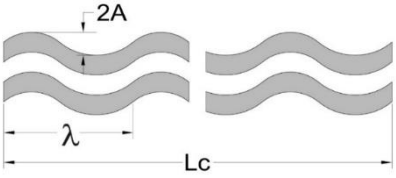

Figure 5. The top view of the wavy micro-channel

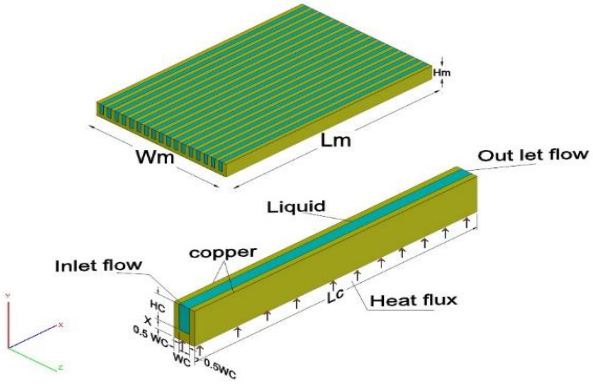

Figure 6. (a) Geometry of zigzag microchannel heat sink, (b) Geometry of (ZMHS) unit.

This work investigates a zigzag microchannel heat sink (ZMHS), as depicted in Fig. 6. The ZMHS has seventeen zigzag units and possesses identical dimensions to a straight microchannel heat sink. The experiment employed a zigzag microchannel angle of 18 degrees, as depicted in Fig. 7.

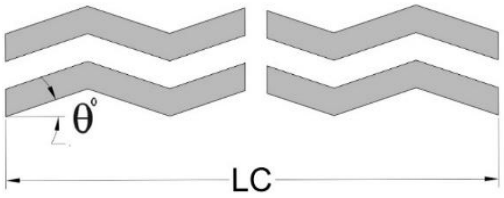

Figure 7. The top view of the zigzag micro-channel.

The present study focuses on the development and analysis of a Microchannel Heat Exchanger with symmetric circular Cavities (MCHS-SCC). Circular cavities were utilized as the primary structural element in this study, as depicted in Fig. 8. The configuration comprised twelve units and possessed identical dimensions to the straight microchannel heat sink. Furthermore, the cavities themselves were circular in shape. The symmetrical circular cavities were measured with a radius of 0.86mm, as illustrated in Fig. 9.

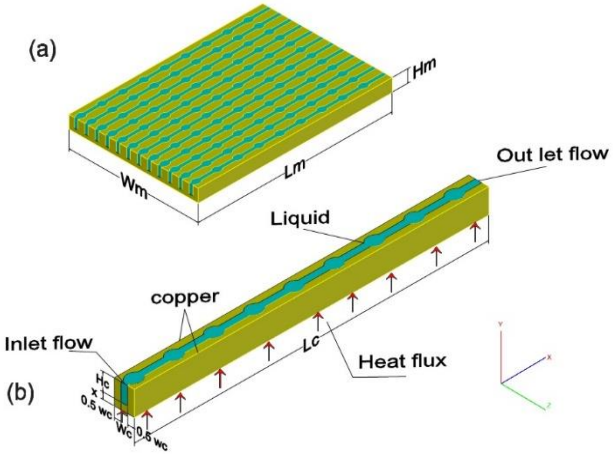

Figure 8. (a) Microchannel Heat Exchangers with symmetric circular Cavities (b). The geometry of (MCHS-SCC) unit.

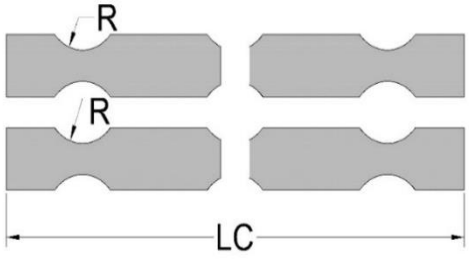

Figure 9. The top view of the Microchannel Heat Exchangers with symmetric circular Cavities.

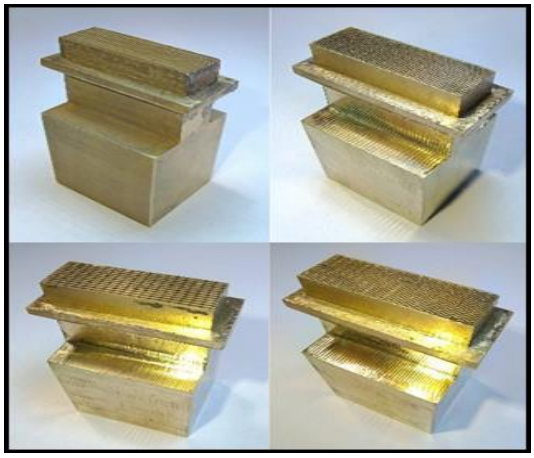

Figure 10. Micro-channels after manufacturin

This study presents a comparative analysis between the published calculations and the current numerical and experimental simulations, focusing on the convergence of results. The validation involved comparing results to experimental results from reference (B. Huang. et al [1].
The model used in this study exhibits good agreement with the experimental findings for temperature-dependent fluid properties, as shown in Fig .11.

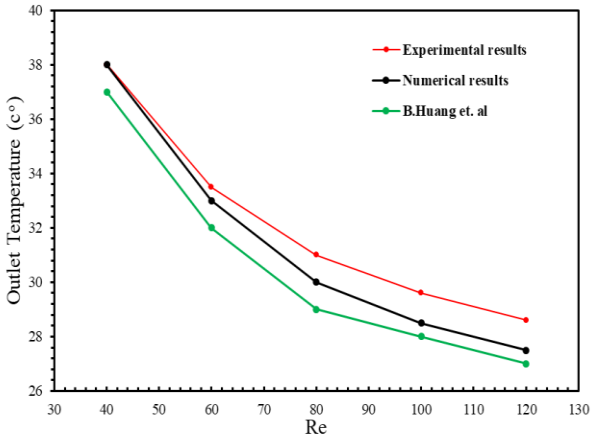

Figure 11. Influence of Re on outlet temperature between the present study and B. Huang. et al [1]

3.1 Governing equations for Cartesian coordinates

Based on the aforementioned assumptions, the governing equations and boundary conditions in the three-dimensional Cartesian coordinate system can be expressed as follows:
Continuity equation for the fluid [23,24]:

$$\frac{\partial u}{\partial u}+\frac{\partial v}{\partial y}+\frac{\partial w}{\partial z}=0 \quad (1)$$

Momentum equations (Navier's Stokes equations) can be written as [25, 26]:

X-momentum equation:

$$u\frac{\partial u}{\partial x}+v\frac{\partial u}{\partial y}+w\frac{\partial u}{\partial z}=-\frac{1}{\rho}\frac{\partial p}{\partial x}+\frac{\mu}{\rho}\left(\frac{\partial^2 u}{\partial x^2}+\frac{\partial^2 u}{\partial y^2}+\frac{\partial^2 u}{\partial z^2}\right) \quad (2)$$

Y-momentum equation:

$$u\frac{\partial v}{\partial x}+v\frac{\partial v}{\partial y}+w\frac{\partial v}{\partial z}=-\frac{1}{\rho}\frac{\partial p}{\partial y}+\frac{\mu}{\rho}\left(\frac{\partial^2 v}{\partial x^2}+\frac{\partial^2 v}{\partial y^2}+\frac{\partial^2 v}{\partial z^2}\right) \quad (3)$$

Z-momentum equation:

$$u\frac{\partial w}{\partial x}+v\frac{\partial w}{\partial y}+w\frac{\partial w}{\partial z}=-\frac{1}{\rho}\frac{\partial p}{\partial z}+\frac{\mu}{\rho}\left(\frac{\partial^2 w}{\partial x^2}+\frac{\partial^2 w}{\partial y^2}+\frac{\partial^2 w}{\partial z^2}\right) \quad (4)$$

Energy equation for fluid and solid:

$$u\frac{\partial T_f}{\partial x}+v\frac{\partial T_f}{\partial y}+w\frac{\partial T_f}{\partial z}=\frac{\kappa}{\rho C_P}\left(\frac{\partial^2 T_f}{\partial x^2}+\frac{\partial^2 T_f}{\partial y^2}+\frac{\partial^2 T_f}{\partial z^2}\right) \quad (5)$$

In addition, the expression for the 3D solid-wall steady-state energy equation is:

$$\left(\frac{\partial^2 T_s}{\partial x^2}+\frac{\partial^2 T_s}{\partial y^2}+\frac{\partial^2 T_s}{\partial z^2}\right)=0 \quad (6)$$

3.2 Definition of Nanofluid

A nanofluid is a fluid composed of a base fluid, such as water, oil, or Ethanol glycol, in which nanometer-sized particles, typically fewer than 100 nanometers in size, are uniformly distributed. Nanoparticles, which often have dimensions below 100 nanometers, are uniformly dispersed inside the host fluid. The utilization of nanoparticles holds promise in altering the thermo physical properties of the underlying fluid, including thermal conductivity, viscosity, and specific heat capacity. This study aimed to investigate the application of nanofluids as a cooling medium in order to improve the thermal efficiency of a heat sink with microchannels. In this investigation, the nanofluids employed are (CUO-H2O) nanofluids. The volume fractions used are 0.1%, 0.2%, and 0.3% respectively. Table 2 presents the thermo-physical characteristics of nanoparticles [27,28].

Table 2. The thermophysical characteristics of Base Fluid (pure water) and nanoparticles

Thermophysical characteristics	ρ (kg/m3)	cp (J/kgk)	κ (W/mK)
Pure water (H2O) [29]	997.1	4179	0.613
Copper oxide (CuO) [30]	6500.0	535.6	20.00

3.3 The numerical simulation

This work used COMSOL Multiphysics to simulate a three-dimensional fluid and heat transport problem in a microchannel. In a microchannel, the fluid flow is often laminar, meaning that the fluid moves in layers without any significant turbulence. This makes it possible to accurately model the flow using computational fluid dynamics (CFD) techniques. The CFD module's complete capabilities include solving stable and unsteady fluid and heat transfer issues in two and three dimensions. The numerical code undergoes many testing methods to ascertain the accuracy and reliability of the numerical analysis. This code used the finite element method to discrete a partial differential equation of pressure, velocity, and temperature.

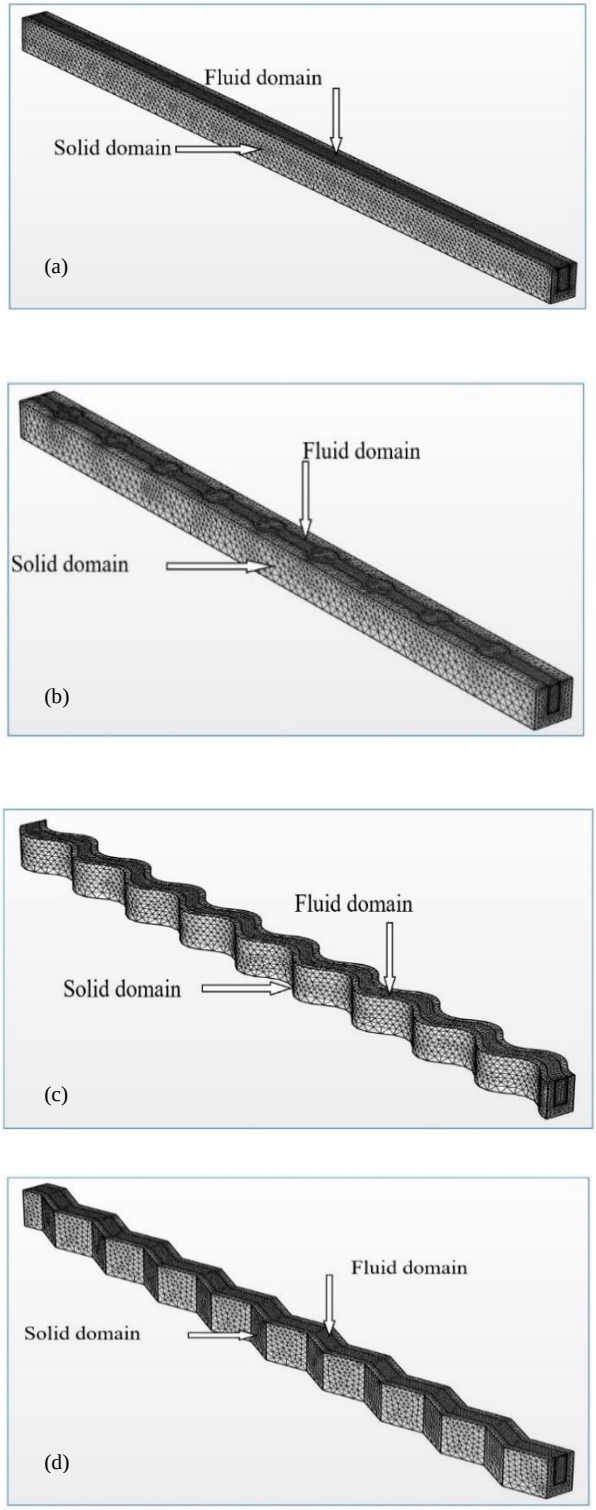

Figure 12. Mesh distribution details for model three dimension (a) straight (b) circular cavities (c) wavy (d) Zigzag channel

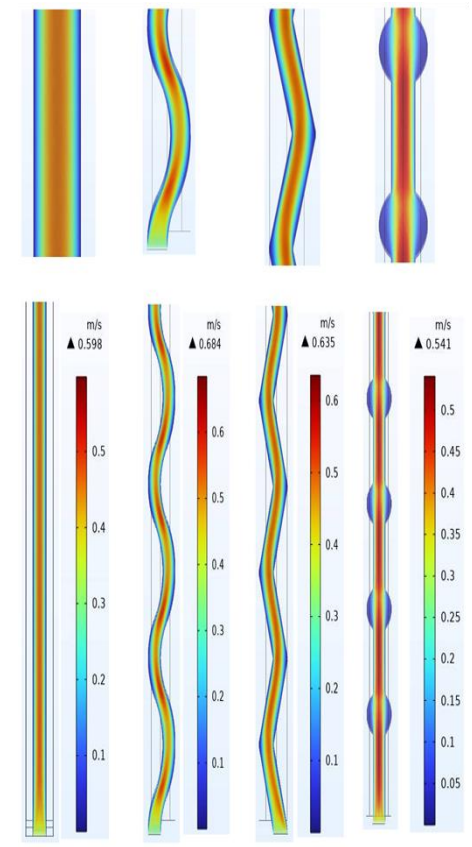

(a) Cuo-H2O nanofluid

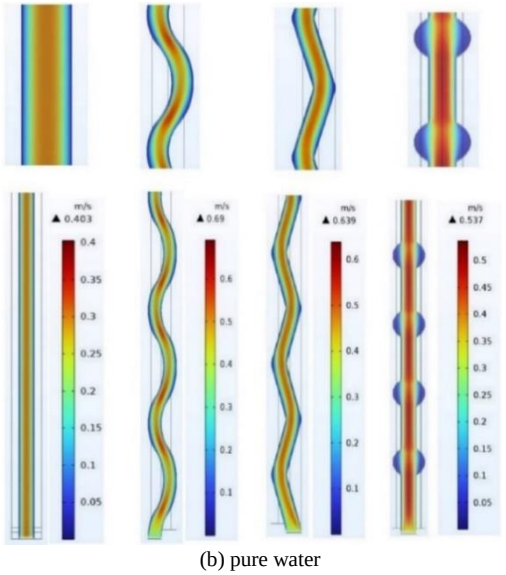

(b) pure water

Figure 13. Illustrates the influence of different microchannel shapes (rectangular, wavy, Zigzag, and circular cavities channel) on the magnitude of velocity, using (a) Cuo-H2O nanofluid and (b) pure water as the working fluid. The Reynolds number (Re) is set at 150, and the heat flux (qw) is maintained at 170 kW/m^2.

4. Results

4.1 Velocity contour characteristics

To investigate the effect of microchannel shapes (straight, Zigzag, wavy, and circular cavities) with rectangular section entrance on velocity magnitude, and due to the similarity of observed behavior, to reduce the number of illustrations, only show one nanoparticle concentration (φ= 0.01), has been selected for Reynolds numbers Re= 150. Fig. 13.

4.2 Temperature contour characteristics

In order to examine heat transfer and compare the various shapes (straight, zigzag, wavy, and circular cavities) utilized in this study, Fig. 14 illustrates the temperature distributions along the micro-channel heat sink for different nanofluid types (CuO-H2O) and a Reynolds number of 150 for pure water. The nanofluid demonstrates a volume concentration of 0.01.

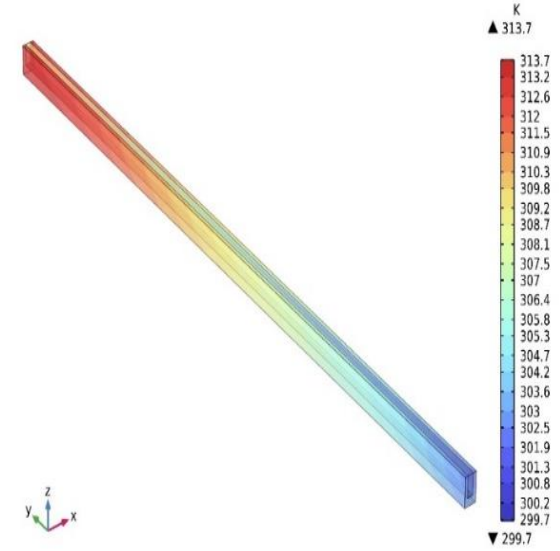

(a)

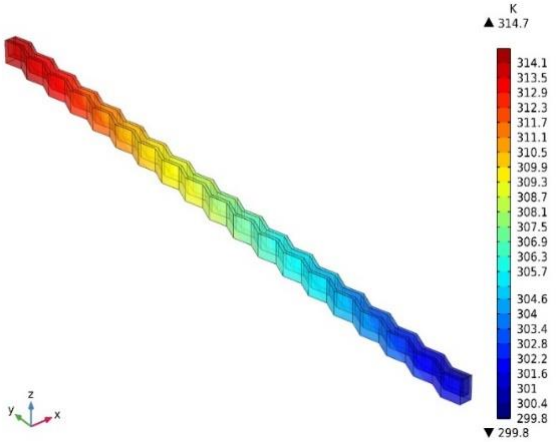

(b)

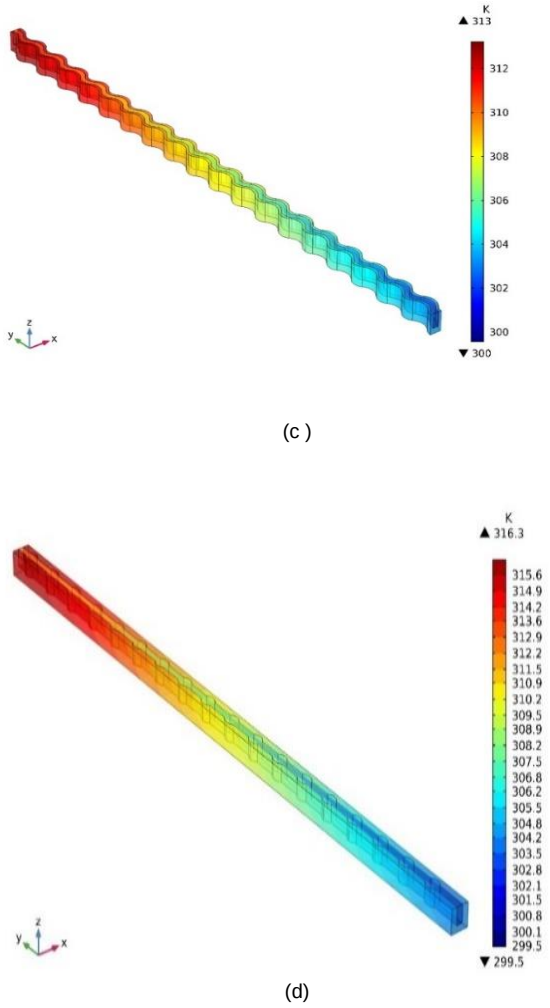

Figure 14. Shows the temperature contour for with pure water work fluid, Re=150, qw=170 kw/m^2 for the micro-channel shapes (a-straight, b-zigzag, c-wavy and d-circular cavities).

4.3 The effect of nanofluids and nanoparticles on microchannel heat sinks.

The thermal resistance of a microchannel heat sink is dependent on two factors: the coolant's inlet temperature and the highest temperature recorded at the heat sink's wall. The figures below present the thermal resistance (k/w) of the straight microchannel and different channels (zigzag, wavy, and circular cavities) studied in the search.

4.4 Comparison of experimental and numerical results

The obtained experimental results were then compared to the numerical results, exposing a significant level of agreement, as depicted in Fig.15. Error rates ranged from 1.2% to 5.2% when using distilled water as a coolant. However, when Nanofluid was used as a coolant, the error rate varied between (0.75% and 4.9%). Comparisons between experimental and numerical Nusselt Number (Nu) results for all channels (straight, Wavy, Zigzag, and circular cavities) are depicted in Fig. 16. When using Nanofluid and distilled water as a coolant, a similar general behavior and apparent convergence in the results were observed, as the largest deviation between numerical and experimental Nusselt number values was (2.6-9.8%). These results suggest that as flow rates increase, the temperature of the wall decreases while the Nusselt number increases. Figures 10 and 11 below show the evolution of the friction factor with the Reynolds number for the straight Microchannel and different channels (zigzag, wavy, and circular cavities) studied in the search.

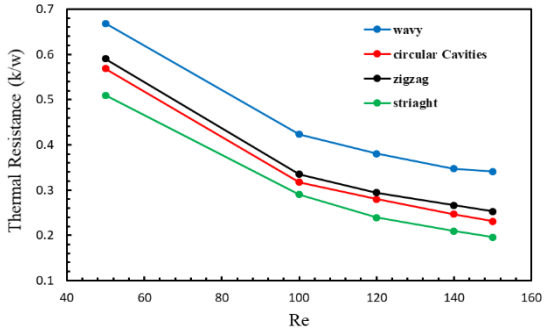

Figure 15. Shows the Thermal Resistance (k/w) of the different channels at q = 170kw/m^2 using (0.01cuo-H2O).

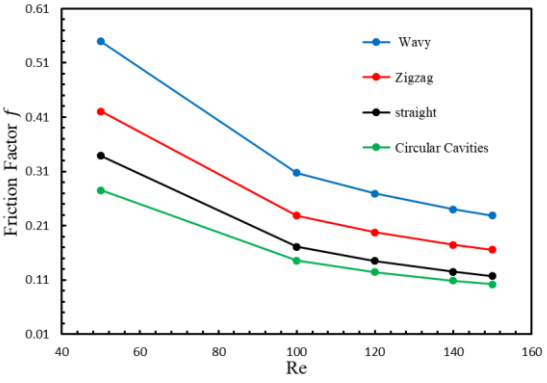

Figure 16. Shows the effect of used (CUO-H2O) nanofluid volume concentrations (φ) (0.01%) as a coolant on friction factor (f) in the different channels at q=170kw/m^2.

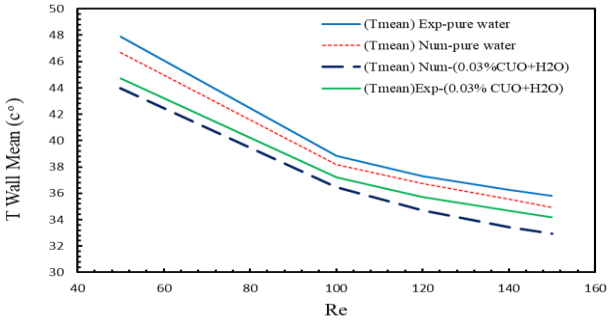

Figure 17. Shows the comparisons between numerical and experimental results of the wall temperature of the Straightmicro heat sink .

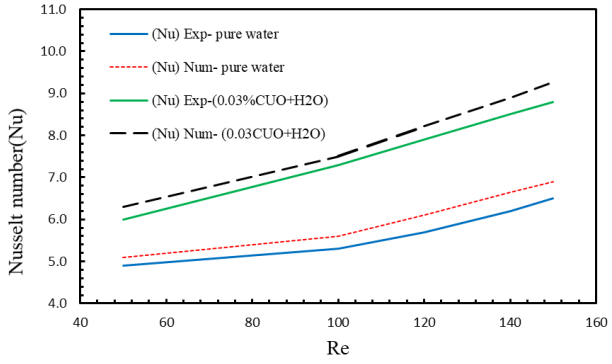

Figure 18. Shows the comparisons between numerical and experimental results of the local Nusselt number of Straight micro-channel heat sinks.

5. Conclusions

1. The results elucidated that the pressure drop increases when the geometry of the channel alters and 'with the increase of both the Reynolds number and the nanoparticle volume concentration. The results indicated that the wavy micro-channel heat sink achieved the highest readings compared to the other channels used in the research. In addition, the circular cavities channel heat sink obtained the lowest readings.
2. The thermal resistance decreased at all values of all the Reynolds.
3. Numbers and all the concentrations of nanoparticles used in the search, where the relationship is inverse with it. Moreover, the results showed that the straight microchannel heat sink achieved the lowest readings of thermal resistance compared to the other microchannels.
4. The findings indicated that the friction factor decreases with an increase in the Reynolds number, and it increases as 'the volumetric concentration of nanoparticles rises. It is noted that there is a discrepancy in the results where the channel geometry has a role in that.
5. The Experimental results revealed that Nusselt's Number exhibits an upward trend as the Reynolds number increases across various channel geometries and working fluids under investigation. Furthermore, the utilization of nanofluids as a coolant, as opposed to pure water, leads to an increase in the Nusselt's Number. Also, the wavy microchannel heat sink recorded the highest results. And Nusselt's Number is positively proportional to the increase in the volumetric concentration of the nanoparticles used in the current study.
6. The experimental and numerical results indicated that The findings that the mean wall temperature was found to be reduced at all the (rectangular, wavy, Zigzag, and circular cavities) microchannel heat sink as a result of increasing the flow rate and utilizing nanofluids. The lowest mean wall temperature recorded from the experimental results was 34.2 c° at the (CuO–H2O) nanofluid with a volume fraction of 0.03, at a heat flux value 170kw/m2, and a Reynolds number (Re) of 150. Additionally, the highest mean wall temperature recorded was when using (the circular cavities) micro-channel heat sink 53.2 c°, with when pure water was a coolant, at heat flux value 170kw/m2, and a Reynolds number (Re) 150.
7. The experimental and numerical results showed that the cooling performance is better for all microchannels studied in this study when using nanofluids, and it increases as 'the volumetric concentration of nanoparticles increases and at all heat flux values.
8. The investigation focused on examining the impact of copper oxide nanoparticles on thermal conductivity. An enhancement in thermal conductivity was observed as the concentration of nanoparticles increased. Additionally, it was observed that decreasing the particle size led to an enhancement in the thermal conductivity of the fluids. A reduction in the dimensions of nanoparticles results in an augmentation of the Brownian motion exhibited by the particles. The low viscosity of the fluids is thought to contribute to increased reinforcement. The subsequent study will be about studying the effect of phase change material (PCM) and NCPCM as cooling medium.

Authors' contribution

All authors contributed equally to the preparation of this article.

Declaration of competing interest

The authors declare no conflicts of interest.

Funding source

This study didn't receive any specific funds.

Data availability

The data that support the findings of this study are available from the corresponding author upon reasonable request.

REFERENCES

[1] Binghuan Huang , Haiwang Li, Shuangzhi Xia, and Tiantong , Experimental investigation of the flow and heat transfer performance in micro-channel heat exchangers with cavities , International Journal of Heat and Mass Transfer, 2020. 159: p. 1-10. https://doi.org/10.1016/j.ijheatmasstransfer.2020.120075

[2] Xiaoxin Zeng, Hao Yu, Tianbiao He, and Ning Mao, A Numerical Study on Heat Transfer Characteristics of a Novel Rectangular Grooved Microchannel with Al2O3/Water Nanofluids, Energies, 2022. 15: p. 1-18. https://doi.org/10.3390/en15197187

[3] Marc Hodes, Randy D.Weinstein, Stephen J. Pence, and Jason M. Piccini, Transient thermal management of a handset using phase change material (PCM), Journal of Electronic Packaging, 2002. 124(4): p. 419-426. http://dx.doi.org/10.1115/1.1523061

[4] Steinke, M. E., & Kandlikar, S. G. (2006). Single-phase liquid friction factors in microchannels. International journal of thermal sciences, (2006), 45(11), 1073-1083. https://doi.org/10.1016/j.ijthermalsci.2006.01.016

[5] Seo Young Kim, Jin Wook Paek, and Byung Ha Kang , Thermal performance of aluminum-foam heat sinks by forced air cooling , IEEE Transactions on Components and Packaging Technologies, 2003. 26(1): p. 262-267. https://doi.org/10.1109/TCAPT.2003.809540

[6] Hamidreza Shabgard, Michael J. Allen, Nourouddin Sharifi, Steven P. Benn, Amir Faghri, and Theodore L. Bergman, Heat pipe heat exchangers and heat sinks: Opportunities, challenges, applications, analysis, and state of the art , International Journal of Heat and Mass Transfer, 2015.89: p. 138-158. https://doi.org/10.1016/j.ijheatmasstransfer.2015.05.020

[7] Prajapati, Y. K. , Influence of fin height on heat transfer and fluid flow characteristics of rectangular microchannel heat sink. International Journal of Heat and Mass Transfer, (2019),137, 1041-1052. https://doi.org/10.1016/j.ijheatmasstransfer.2019.04.012

[8] Peng, M., Chen, L., Ji, W., & Tao, W. , Numerical study on flow and heat transfer in a multi-jet microchannel heat sink. International Journal of Heat and Mass Transfer, (2020), 157, 119982. https://doi.org/10.1016/j.ijheatmasstransfer.2020.119982

[9] Ravi Kandasamy, Xiang-Qi Wang, and Arun S. Mujumdar, Transient cooling of electronics using phase change material (PCM)-based heat sinks ,

Journal of Applied Thermal Engineering , 2008 . 28(8): p. 1047-1057. https://doi.org/10.1016/j.applthermaleng.2007.06.010

[10] Mohammada, D.A., Hasana, M.I. and Shkaraha, A.J., Numerical investigation of the electric double-layer effect on the performance of microchannel heat exchanger at combined electroosmotic and pressure-driven flow. Al-Qadisiyah Journal for Engineering Sciences, 2021, 14(1). https://qjes.qu.edu.iq/article_179119.html

[11] Lafta TBENA, H., & Ismael HASAN, M., Numerical investigation of microchannel heat sink with MEPCM suspension with different types of PCM. AL-Qadisiyah Journal for Engineering Sciences, (2018), 11(1), 115-133. https://doi.org/10.30772/qjes.v11i1.524

[12] Hasan, M. I., Study of microchannel heat sink performance with expanded microchannels and nanofluids. AL-Qadisiyah Journal for Engineering Sciences, (2016), 9(4), 426-445 https://qjes.qu.edu.iq/article_118948.html

[13] Aris, M. S. et. al., The development of active vortex generators from shape memory alloys for the convective cooling of heated surfaces , International journal of heat and mass transfer, 2011.54: p. 15-16. https://doi.org/10.1016/j.ijheatmasstransfer.2011.03.030

[14] Mudawar, I. , Assessment of high-heat-flux thermal management schemes , IEEE transactions on components and packaging , 2001. 4(2): p. 122-141. https://doi.org/10.1109/6144.926375

[15] Harshal Gugarathi, Use of nanoparticle enhanced phase change material (NEPCM) for data center cooling application, University of Texas , 2014 . A thesis for the degree of Master of Science in Mechanical Engineering. http://hdl.handle.net/10106/26707

[16] Abdelmalek, Z., D'Orazio, A., & Karimipour, A. The effect of nanoparticle shape and microchannel geometry on fluid flow and heat transfer in a porous microchannel. Symmetry, (2020), 12(4), 591. https://doi.org/10.3390/sym12040591

[17] Manay, E., & Sahin, B., Heat transfer and pressure drop of nanofluids in a microchannel heat sink. Heat Transfer Engineering, (2017)., 38(5), 510-522. https://doi.org/10.1080/10407782.2016.1195162

[18] Bahiraei, M., & Monavari, A., Impact of nanoparticle shape on thermohydraulic performance of a nanofluid in an enhanced microchannel heat sink for utilization in cooling of electronic components. Chinese Journal of Chemical Engineering, (2021),40, 36-47. https://doi.org/10.1016/j.cjche.2020.11.026

[19] Adio, S. A., Alo, T. A., Olagoke, R. O., Olalere, A. E., Veeredhi, V. R., & Ewim, D. R., Thermohydraulic and entropy characteristics of Al2O3-water nanofluid in a ribbed interrupted microchannel heat exchanger. Heat Transfer, (2021), 50(3), 1951-1984. https://doi.org/10.1002/htj.21964

[20] Al-Baghdadi, M. A. S., Noor, Z. M., Zeiny, A., Burns, A., & Wen, D. , CFD analysis of a nanofluid-based microchannel heat sink. Thermal Science and Engineering Progress, (2020), 20, 100685. https://doi.org/10.1016/j.tsep.2020.100685

[21] Eneren, P., Aksoy, Y. T., & Vetrano, M. R. , Experiments on single-phase nanofluid heat transfer mechanisms in microchannel heat sinks: a review. Energies, (2022) , 15(7), 2525. https://doi.org/10.3390/en15072525

[22] Rimbault, B., Nguyen, C. T., & Galanis, N., Experimental investigation of CuO–water nanofluid flow and heat transfer inside a microchannel heat sink. International Journal of Thermal Sciences, (2014), 84, 275-292. http://dx.doi.org/10.1016/j.ijthermalsci.2014.05.025

[23] F. M. White, Viscous Fluid Flow , Third Edition, University of Rhode lsland, 2021. https://doi.org/10.1201/9780367802424

[24] Ali, A. A., Hasan, M. I., & Adnan, G. , Numerical investigation of rougness effects on hyderdynmic and thermal performance of counter flow microchannel heat exchanger. Al-Qadisiyah Journal for Engineering Sciences, (2018), 11(4), 426-445. https://doi.org/10.30772/qjes.v11i4.571

[25] Barik, A. M., & Al-Farhany, K., Numerical Investigation of the effect of baffle inclination angle on nanofluid natural convection heat transfer in a square enclosure. Al-Qadisiyah Journal for engineering sciences, (2019), 12(2), p. 61-71. https://doi.org/10.30772/qjes.v12i2.589

[26] Vasilev, M. P., Abiev, R. S., & Kumar, R., Effect of circular pin-fins geometry and their arrangement on heat transfer performance for laminar flow in microchannel heat sink. International Journal of Thermal Sciences, (2021), 170, 107177. https://doi.org/10.1016/j.ijthermalsci.2021.107177

[27] Al-Ali, H. M., & Hamza, N. H. The effect of ribs spacing on heat transfer in rectangular channels under the effect of different types of heat flux in the Presence of a nanofluids,(2021),14, p 95-103. https://doi.org/10.30772/qjes.v14i2.756

[28] Nura Mu'az Muhammad , Nor Azwadi Che Sidik, Aminuddin Saat, and Bala Abdullahi , Effect of Nanofluids on Heat Transfer and Pressure Drop Characteristics of Diverging-Converging Minichannel heat sink , CFD Letters, (2019), 4: p. 105 -120. https://doi.org/10.1007/s00231-017-1978-7

[29] Assel Sakanova. et. al. , Performance improvements of microchannel heat sink using wavy channel and nanofluids , International Journal of Heat and Mass Transfer, (2015), 89: p. 59-47. https://doi.org/10.1016/j.ijheatmasstransfer.2015.05.033